11th International Symposium on Turbulence and Shear Flow Phenomena (TSFP11)
Southampton, UK, July 30 to August 2, 2019

IN SEARCH OF LOW DRAG EVENTS IN NEWTONIAN TURBULENT CHANNEL FLOW AT LOW REYNOLDS NUMBER

Rishav Agrawal
School of Engineering
University of Liverpool
Liverpool L69 3GH, UK
rishavag@liverpool.ac.uk

Henry C.-H. Ng
School of Engineering
University of Liverpool
Liverpool L69 3GH, UK
hchng@liverpool.ac.uk

Richard D. Whalley
School of Engineering
Newcastle University
Newcastle NE1 7RU, UK
richard.whalley@ncl.ac.uk

David J. C. Dennis
School of Engineering
University of Liverpool
Liverpool L69 3GH, UK
djcd@liverpool.ac.uk

Robert J. Poole
School of Engineering
University of Liverpool
Liverpool L69 3GH, UK
robpoole@liverpool.ac.uk

ABSTRACT

Recent Direct Numerical Simulations (DNS) and experiments in turbulent channel flow have found intermittent low drag behaviour in Newtonian fluid flows, between friction Reynolds numbers 70 and 100, whose mean streamwise velocity profile approaches the Virk Maximum Drag Reduction (MDR) asymptote; a profile which is more routinely associated with turbulent flows containing a drag-reducing additive. These intervals of low drag have been termed "hibernating turbulence" and in this experimental investigation, further verification of the hibernating turbulence phenomena is investigated in a channel flow facility using Newtonian fluids. Simultaneous measurements of instantaneous streamwise and wall-normal velocities, and wall shear stress are conducted using Laser Doppler Velocimetry (LDV) and Hot-film Anemometry (HFA), respectively. Experiments are conducted at friction Reynolds number of 70 for 10 different wall-normal locations. The effect of varying the criteria for a hibernating event on the ensemble-averaged wall shear stress during hibernation is investigated. Velocity data obtained during the low drag events are conditionally-averaged and normalized using two different values of mean wall shears stress: long time-averaged wall shear stress and conditionally-averaged wall shear stress. It is observed that the conditionally-averaged streamwise velocity when normalized with the conditionally-averaged wall shear stress approaches Virk MDR asymptote closer to the wall. There is found to be a decrease in the conditionally-averaged Reynolds shear stress (RSS) near the wall when the normalization is based on long time-averaged wall shear stress.

INTRODUCTION

The discovery of travelling-wave solutions for the Navier Stokes equation have greatly advanced our understanding of canonical shear flows. These travelling-wave solutions are three dimensional and non-linear and are also sometimes called Exact Coherent States (ECS) (Waleffe, 2001). Mostly, these ECS solutions are observed to occur in pairs at saddle-node bifurcations where the upper branch solution is found to have higher velocity fluctuation and higher drag than the lower branch solution. Park & Graham (2015) used DNS in minimal channel geometry to find new ECS solutions, which they denote as the "P4" solution. The velocity profile of the upper branch of this solution approaches the classic Prandtl-von Kármán log-law, while the velocity profile of the lower branch approaches the Virk MDR asymptote (Virk, 1975). This MDR asymptote is generally associated with viscoelastic turbulent flows which is believed to be independent of polymer concentration or Reynolds number (Virk, 1975). The existence of such solutions for Newtonian flows opens a window of opportunity with potentially significant practical implications. These intermittent moments of higher drag and lower drag in turbulent flows were given the nomenclature of "active" and "hibernating" turbulence by Xi & Graham (2012). Kushwaha *et al.* (2017) extended the work by conducting temporal analyses for minimal channels and spatiotemporal analyses for extended domains and finding relationships between the two. They found that for $Re_\tau = u_\tau h/\nu$ between 70 and 100, during the low-drag events, the localized near-wall flow structure and the conditional mean velocity profiles for $y^+ = yu_\tau/\nu < 30$ resembles the lower branch of the P4 ECS solution (where u_τ, h, ν, y represent friction velocity, channel half-height, kinematic viscosity and wall-normal distance, respectively). Whalley *et al.* (2017) provided the first experimental verification of this so-called hibernating turbulence for channel flows and it was found that the conditional mean velocity during low-drag events is in good agreement with the P4 ECS solution obtained for a minimal domain. Park *et al.* (2018) related the strong turbulent bursts to the hibernating turbulence in the minimal channel flow where they showed that many hibernating events are followed by strong turbulent bursts. RSS characteristics during hibernation is studied in minimal channel flow using DNS by Xi & Graham (2012) and Park & Graham (2015), where it is observed that RSS drops to a low value during hibernation. In the present work, an experimental study of RSS characteristics during hibernation is

carried out in a channel flow facility.

EXPERIMENTAL SET-UP

The channel flow facility used in this study has a similar arrangement to that used by Whalley *et al.* (2017) in our laboratory. A schematic representation of the channel flow facility is shown in figure 1. The channel consists of 6 stainless steel modules and a test section, which is connected at the downstream of five stainless steel modules. Each module is of length 1.2 m and the test section has a length of 0.25 m. The full-width ($2w$) and full-height ($2h$) of the duct are 0.298 m and 0.025 m, giving an aspect ratio (w/h) of 11.92. The top and side walls of the test section are made of borosilicate glass, from where the LDV measurements can be conducted. A water and glycerine mixture (Newtonian fluid) is used as the working fluid. A Mono type E101 progressive cavity pump is used to circulate the fluid via a stainless steel header tank in the closed loop, where the fluid passes through three pulsation dampeners before entering the channel. A Platinum Resistance Thermometer (PRT), located inside the last downstream module of the working section, is used to measure the ambient fluid temperature. Bulk velocity is measured using a Promass Coriolis flow meter which is installed in the return loop. Pressure-drop measurements are conducted between two pressure tappings across a distance of $164h$ using a Druck LPX-3981 differential pressure transducer which has a working range of 5 kPa and an accuracy of ± 5 Pa, where the upstream pressure tap is 408 channel half-heights away from the inlet of the channel.

Instantaneous streamwise and wall-normal velocity measurements are made using a Dantec FibreFlow LDV system. Calculation of RSS requires simultaneous measurements of streamwise and wall-normal velocities, which cannot be obtained at the near-wall region of the mid-spanwise location of the channel due to cut-off of the beam near the wall (Poggi *et al.*, 2002). To reach closer to the bottom wall, the measurement location is moved closer to the side wall. To investigate the effect of side walls, streamwise velocity profiles were measured for varying spanwise locations of $z/h = 2$ to $z/h = 8$ for $Re_\tau = 78$, where z indicates distance from the side-wall. Figure 2 shows the mean velocity profiles measured for various spanwise locations, where $\overline{U}^+ = \overline{U}/u_\tau$ and $y^+ = yu_\tau/\nu$, and $\overline{U}$ indicates time-averaged streamwise velocity. It is observed that the mean velocity profiles approach an asymptote after a spanwise location of $z/h = 4$. Vinuesa *et al.* (2015) studied the effect of side walls for channel flows of finite aspect ratios using DNS. They found that the kinetic energy of the secondary flow for the aspect ratio of 10 at $Re_\tau \approx 180$ decays to approximately zero after spanwise location of 4 channel half-heights from the side wall. Based on the DNS results by Vinuesa *et al.* (2015) and the present experimental results, it is inferred that the spanwise location of 5 channel half-heights from the side wall satisfies the 2-D channel approximation for our channel facility.

The next modification made is to rotate the laser head by 45° along the spanwise direction to go closer to the bottom wall. Velocity components $\pm 45^o$ to the streamwise and wall-normal axis are measured using two pairs laser of beams. Streamwise and wall-normal velocity components are then calculated using trigonometric relations. Similar rotation of the laser head for LDV measurements have been done previously by Melling & Whitelaw (1976) and Walker & Tiederman (1990) in channel flows. An external bi-concave lens, aligned with the laser beams, is also attached to the laser head of the LDV to increase the focal length of the beams from 160 mm to 370 mm in air. This provides us an opportunity to measure even closer to the bottom wall. The LDV is operated in forward scatter mode and the typical data rates are around 100 Hz depending on the signal gain employed. Using these approaches we are able to measure the RSS from a distance of $y/h \simeq 0.3$ at $z/h = 5$.

Hot-film anemometry is employed to measure instantaneous wall shear stress where a Dantec 55R48 glue-on hot-film probe is used as the sensor. A hot-film probe having streamwise and spanwise lengths (in viscous units) of 0.58 and 5.3 for $Re_\tau = 70$ is glued at a spanwise location of $z/h = 5$ from the side wall. The probe is powered by a Dantec StreamLine Pro velocimetry system and is operated under constant temperature (CT) mode. Hot-film calibration is conducted against mean pressure-drop, measured using the pressure transducer. To avoid any thermal drift in the output voltage, the temperature of the working fluid is controlled to a precision of $\pm$ 0.02° C for the entire experimental run using a heat exchanger (typically 2 hours). Figure 3 shows an example of hot-film calibration conducted using pressure transducer. A third order polynomial is used to fit the calibration points.

In the present study, wall shear stress and velocity measurements are conducted simultaneously at $Re_\tau = 70$. This Reynolds number is chosen for the current study because this is the lowest Reynolds number where the evidence of hibernating turbulence is shown by previous researchers: Kushwaha *et al.* (2017) and Whalley *et al.* (2017) in extended domains and it gives us the opportunity to measure closer to the bottom wall in inner units compared to higher Reynolds numbers. Recently, using two-point spa-

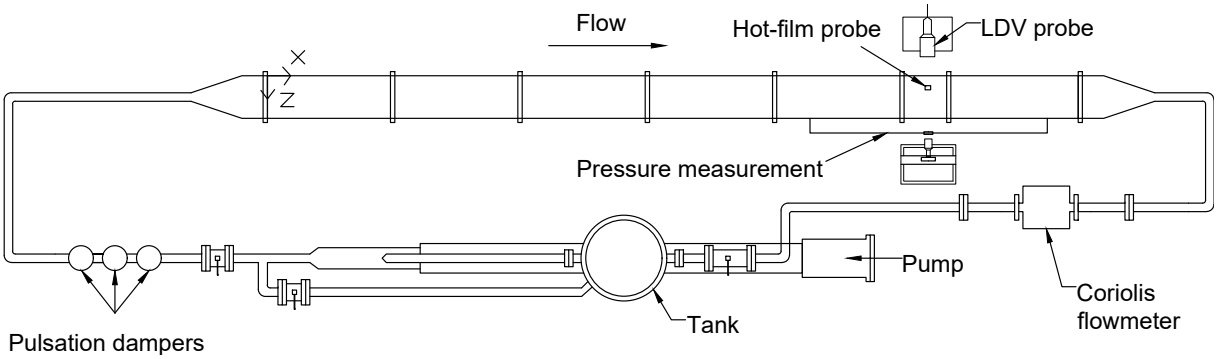

Figure 1: Schematic of the experimental rig (not to scale), flow is clockwise.

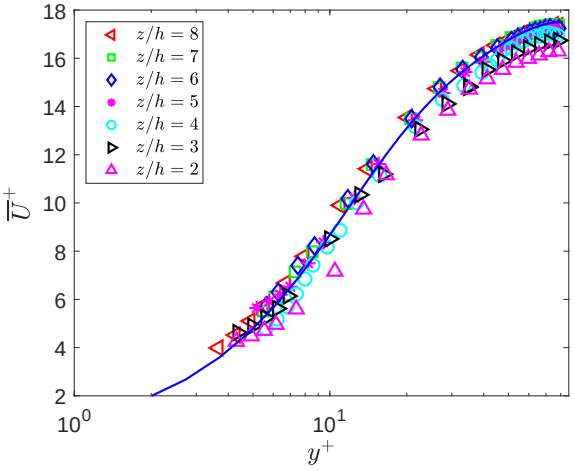

Figure 2: Normalized streamwise velocity profiles for $Re_\tau = 78$ for spanwise locations of two channel half-heights to eight channel half-heights from the side-wall. DNS profile obtained from Kushwaha *et al.* (2017) for Re_τ = 80 is shown by a blue solid line.

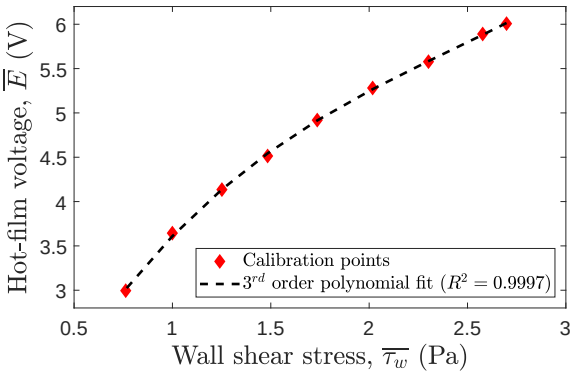

Figure 3: Example of a hot-film calibration curve for $Re_\tau = 70$. The calibration data is fit with a third-order polynomial.

tial correlation of wall shear stress we also observed that the large-scale intermittency of laminar-turbulent transition disappears in our channel flow by $Re_\tau \sim 60$. The streamwise and spanwise locations of the measurements are $x/h = 496$ and $z/h = 5$, respectively, where x is the distance from the inlet of the channel. The flow is sampled for 10 different wall normal locations, y^+ = 21.1, 24.0, 27.8, 31.8, 35.4, 40.1, 47.4, 52.9, 61.1, 68.2 where each wall-normal location is sampled for 2 hours.

RESULTS AND DISCUSSION

Figure 4 shows the distribution of all the negative wall shear stress fluctuations (i.e. below the mean, $\overline{\tau_w}$) per hour for various time durations of occurrence. In the present study, the criteria to detect a hibernating event is that the instantaneous wall shear stress should drop to 90% of the long time-averaged wall shear stress and stay there for a minimum non-dimensional time duration $t^*(= tu_\tau/h)$ of 3, which is also the criteria used by Kushwaha *et al.* (2017) and Whalley *et al.* (2017). The solid black lines in figure 4 show the threshold criteria and time duration criteria for a hibernating event. So, it can be said that the hibernating events are a subset of low wall shear stress events with a threshold and a time duration criteria. Later, the effect of changing these two criteria are also discussed. Data are collected for two hours using LDV and HFA simultaneously to characterize the hibernating events for each wall normal location. All the low wall shear stress events which meet the above criteria are conditionally sampled and ensemble-averaged. LDV acquires data at random intervals due to random arrival times of particles in the measurement volume (Benedict *et al.*, 2000). Therefore, the time series obtained are distributed at uneven time intervals. To carry out the ensemble averaging of the instantaneous velocities and wall shear stress the time histories are interpolated to a constant time step. In the present work, a sample and hold interpolation method is used for the resampling of unevenly distributed data. In this method, the sampled quantity is assumed to be constant until a new sample indicates that the value has changed. The resampling frequency is kept to be 100 Hz, which is in the same range as the actual average acquisition frequency. Figure 5(a) shows the instantaneous wall shear stress normalized by the long time-averaged wall shear stress for 1590 hibernating events obtained for Re_τ = 70. All the curves are shifted so that $t^* = 0$ marks the beginning of the hibernating events. The ensemble-averaged wall shear stress (as shown by a solid blue line) drops to about 70% of the long time-averaged wall shear stress during hibernation. There is found to be a good agreement of the ensemble-averaged wall shear stress obtained by Kushwaha *et al.* (2017) and Whalley *et al.* (2017) with the present experiment. An attempt is also made to study the effect of changing the threshold and time duration criteria for hibernation on the ensemble-averaged wall shear stress. Four different threshold criteria: $\tau_w/\overline{\tau_w} < 0.8$, 0.85, 0.9 and 0.95 and two different time duration criteria: $t^* > 2$ and 3 are considered for this study. From figure 5(b) it is observed that making the threshold criteria more stringent from 0.95 to 0.8 decreases the value of ensemble-averaged wall shear stress during the low drag events. Changing the time duration criteria from t^* from 2 to 3 doesn't change the value of the ensemble-averaged wall shear stress although the hibernation duration becomes smaller. Very similar results were also obtained by Kushwaha *et al.* (2017) in channel flow using DNS for $Re_\tau = 100$.

As mentioned previously, simultaneous measurements of velocities using LDV above the hot-film are made for various wall-normal locations. This enables us to conduct conditional sampling of the velocity data during the low drag events. Figure 6 shows the ensemble-averaged streamwise velocities (U), wall-normal velocities (V) and negative uv for three wall normal locations for $Re_\tau = 70$, where u and v are the streamwise and wall-normal velocity fluctuations and the time average of negative uv gives RSS ($-\overline{uv}$). All the ensemble-averaged quantities are normalized by the long time-averaged friction velocity. From figure 6(a) it is observed that the there is a decrease in the ensemble-averaged streamwise velocity during the low-drag events for various wall-normal locations but the effect seems to diminish closer to the centreline. Figure 6(b) shows that away from the low-drag events the mean wall-normal velocity is close to zero, but during the low drag events there is an increase in the wall-normal velocity which is observed to be significant even near the centreline. Figure 6(c) shows that the ensemble-averaged negative uv decrease during the low drag event for lower y^+ but becomes insensitive closer to the centreline. After en-

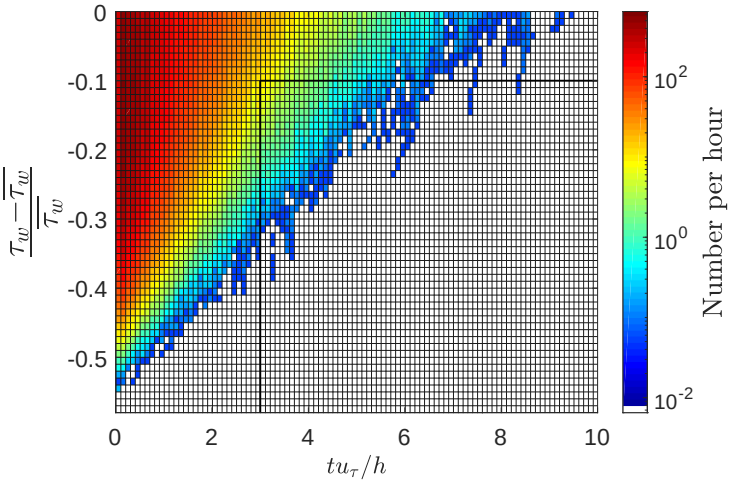

Figure 4: Number of negative wall shear stress fluctuations per hour as a function of threshold and duration criteria for $Re_\tau = 70$. The black lines cover the region of low-drag "hibernating" events based on the present criteria on time duration and the threshold.

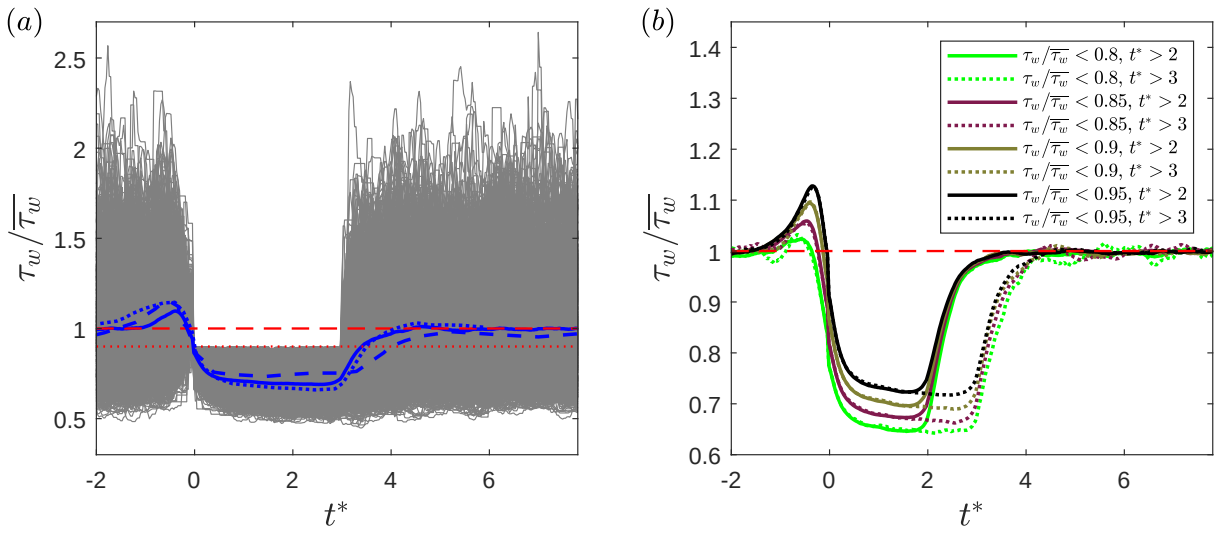

Figure 5: (a) Instantaneous normalized wall shear stress (thin grey lines; 1590 events) during low drag events and ensemble-averaged wall shear stress (thick blue line) during low-drag events for $Re_\tau = 70$. Dotted blue line represents results from Whalley et al. (2017) in a channel flow facility for $Re_\tau = 70$ and dashed blue line represents data obtained using DNS by Kushwaha et al. (2017) for $Re_\tau = 70$. Here, all the time series are shifted so that $t^* = 0$ marks the beginning of hibernating event. Red dashed line represents mean wall shear stress and red dotted line represents the threshold value of $\tau_w/\overline{\tau_w} < 0.9$; (b) Ensemble-averaged wall shear stress during low-drag events for various threshold criteria and time duration criteria for $Re_\tau = 70$.

semble averaging of the instantaneous velocity data during low-drag events, conditional averaging of the velocity data is carried out. To carry out the conditional averaging, events between $0.4 < t^* < t^*_{end} - 0.4$ are considered as low drag events to avoid transient behaviours, where t^*_{end} marks the end of a hibernating event. Conditionally-averaged velocity data and corresponding wall-normal locations are normalized using two different values of mean wall shear stress: long time-averaged wall shear stress and conditionally-averaged wall shear stress. Conditionally-averaged wall shear stress has been used earlier by Whalley *et al.* (2017, 2019) and Kushwaha *et al.* (2017) for the normalization of the conditionally-averaged quantities during low drag events in channel flows. Effect of using two different normalizations are discussed in Xi & Graham (2010). In the present study, the two different normalizations are also used for the other conditionally-averaged quantites: wall-normal velocity (V), root mean square (rms) of the streamwise velocity fluctuations (u_{rms}), rms of the wall-normal velocity fluctuations (v_{rms}) and RSS ($-\overline{uv}$). Figure 7 shows the unconditional and conditional profiles of U, V, u_{rms}, v_{rms} and $-\overline{uv}$ for various wall-normal locations. Figure 7(a) shows unconditional and conditional profiles of streamwise velocity for $Re_\tau = 70$. There is good agreement of the unconditional profiles of streamwise velocity with the DNS profile obtained for channel flow by Kushwaha *et al.* (2017) for $Re_\tau = 70$. The conditional profile where normalization is done using long time-averaged wall shear stress remains below the unconditional profile for lower y^+, and approaches the unconditional mean values near the centreline. This behaviour is also previously discussed in figure 6(a). The conditional profile where normalization is done using

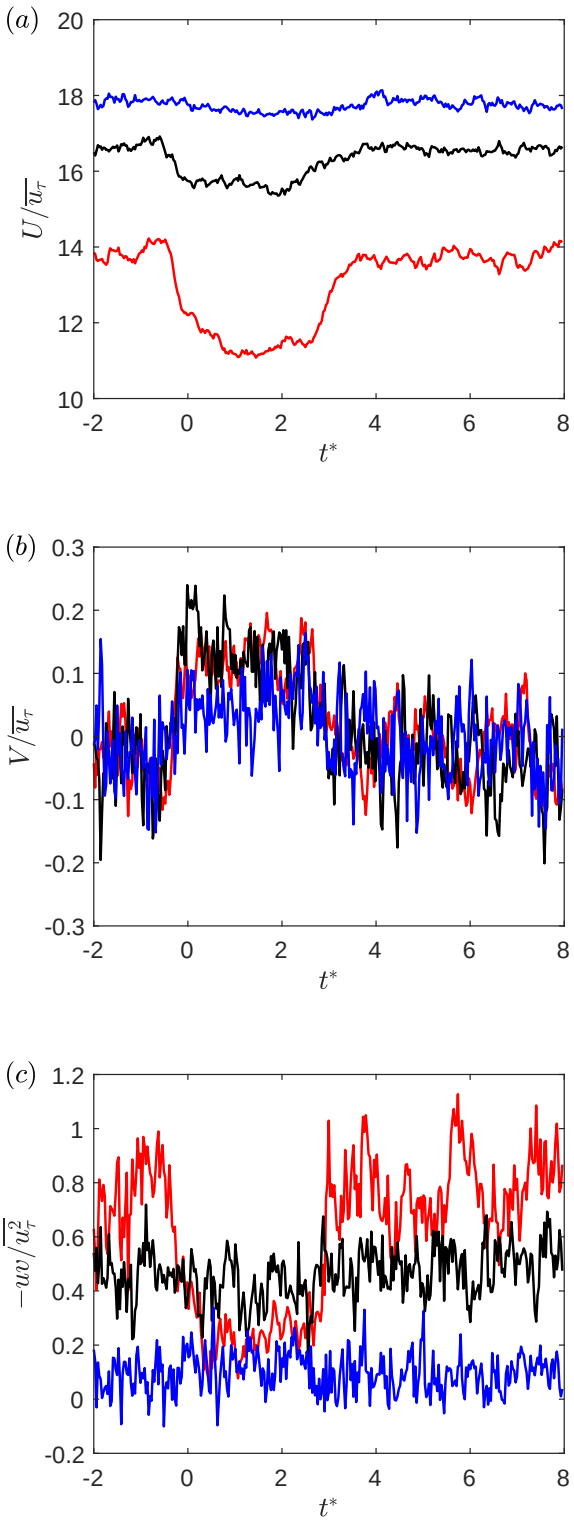

Figure 6: (a) Ensemble-averaged streamwise velocities normalized by the long time-averaged friction velocity during low-drag events for wall-normal locations of y^+ = 21.1 (red line), 40.1 (black line), 68.2 (blue line); (b) Ensemble-averaged wall-normal velocities normalized by the long time-averaged friction velocity during low-drag events where lines represent same quantity as in (a); (c) Ensemble-averaged negative *uv* normalized by the long time-averaged friction velocity during low-drag events where lines represent same quantity as in (a).

conditionally-averaged wall shear stress has higher values than the unconditional profile, which is a consequence of the lower value of ensemble-averaged wall shear stress during hibernation. It can be seen that the conditional profile approaches the 95% confidence interval of Virk MDR log-law for lower y^+ ($y^+ \lesssim 35$) values. A good agreement is also observed with the corresponding conditional profile obtained using DNS by Kushwaha *et al.* (2017) for $Re_\tau = 70$. From figure 7(b), it can be seen that the unconditional wall-normal velocities remain close to zero, but the conditional wall-normal velocities is higher for both normalizations. Error bars in figure 7(b) show the experimental uncertainty associated with the wall-normal velocity measurements. Figure 7(c) shows that the unconditional profile of u^+_{rms} is in good agreement with the DNS data and the conditional profile is lower than unconditional value for $y^+ \lesssim 35$. The unconditional profile of v^+_{rms} is found to be higher than the DNS profile. The higher value of unconditional v^+_{rms} profile is believed to be the consequence of decoupling of the two velocity components from the velocity data obtained using LDV at $\pm 45^o$ orientation. The conditional v^+_{rms}, when the normalized using long time-averaged wall shear stress is found to have lower values than the unconditional profile. Figure 7(d) shows the RSS profiles. There is again found to be a good agreement between the unconditional profiles obtained using DNS and present experiment. The conditional profile, when normalized using long time-averaged wall shear stress is found to have lower values than the unconditional profile for $y^+ \lesssim 35$.

CONCLUSIONS

Simultaneous measurements of velocities and wall shear stress are conducted using LDV and HFA respectively for Re_τ = 70. Hibernating events are shown to be a subset of low wall shear stress events with a threshold and time duration criteria. Ensemble-averaged wall shear stress during hibernation is found be in a good agreement with the previous results obtained using experiments and DNS. The effect of varying the criteria for the threshold and time duration is investigated, and it is seen that making the threshold more stringent reduces the value of ensemble-averaged wall shear stress during hibernation. Decreasing the time duration criteria doesn't change the value of wall shear stress but the duration of hibernation reduces. The conditionally-averaged streamwise velocity profile when normalized with the conditionally-averaged wall shear stress approaches Virk MDR asymptote for lower y^+. The conditionally-averaged RSS profile is observed to have lower values when normalized with the long time-averaged wall shear stress than the unconditional profile for $y^+ \lesssim 35$.

ACKNOWLEDGEMENT

This work has been supported by the Air Force Office of Scientific Research through grant FA9550-16-1-0076. We would like to thank Michael D. Graham and Anubhav Kushwaha for the access to the unconditional DNS profiles.

REFERENCES

Benedict, L. H., Nobach, H. & Tropea, C. 2000 Estimation of turbulent velocity spectra from laser doppler data. *Meas. Sci. Technol.* **11** (8), 1089–1104.

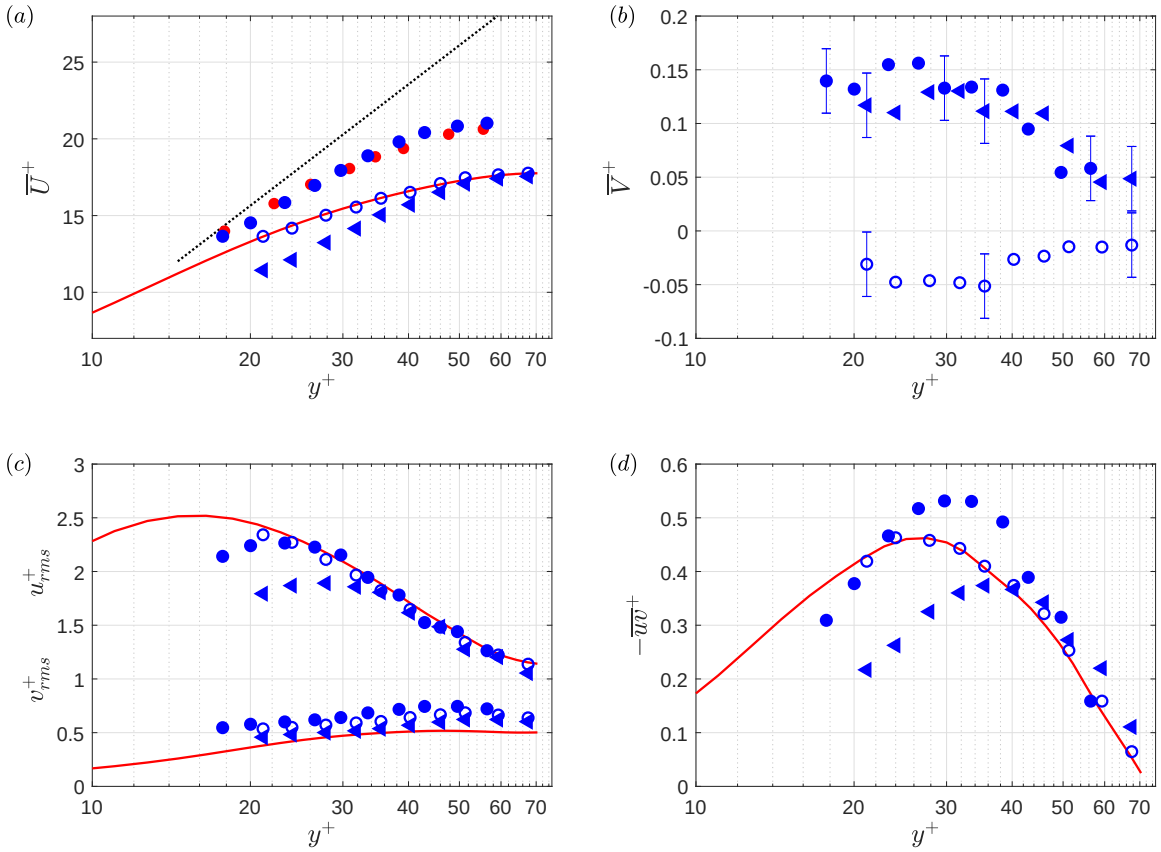

Figure 7: (a) Unconditional (open blue circles) and conditional ensemble-averaged profiles where normalization is conducted based on conditionally-averaged wall shear stress (closed blue circle) and based on long time-averaged wall shear stress (closed blue triangle). Red line and red closed circles show the unconditional and conditionally-averaged streamwise velocity profiles obtained using DNS for $Re_\tau = 70$ (Kushwaha *et al.*, 2017), respectively where normalization for conditional profile is conducted based on conditionally-averaged wall shear stress. Black dotted line shows lower 95% confidence interval of Virk MDR log-law (Kushwaha *et al.*, 2017). (b) Profiles of wall-normal velocity where symbols represent same quantity as in (a). (c) rms profiles of streamwise and wall-normal velocity fluctuations where lines and symbols represent same quantity as in (a). (d) RSS profiles where lines and symbols represent same quantity as in (a).

Kushwaha, A., Park, J. S. & Graham, M. D. 2017 Temporal and spatial intermittencies within channel flow turbulence near transition. *Phys. Rev. Fluids* **2**, 024603.

Melling, A. & Whitelaw, J. H. 1976 Turbulent flow in a rectangular duct. *J. Fluid Mech.* **78**, 289–315.

Park, J. S. & Graham, M. D. 2015 Exact coherent states and connections to turbulent dynamics in minimal channel flow. *J. Fluid Mech.* **782**, 430–454.

Park, J. S., Shekar, A. & Graham, M. D. 2018 Bursting and critical layer frequencies in minimal turbulent dynamics and connections to exact coherent states. *Phys. Rev. Fluids* **3**, 014611.

Poggi, D., Porporato, A. & Ridolfi, L. 2002 An experimental contribution to near-wall measurements by means of a special laser doppler anemometry technique. *Exp. Fluids* **32** (3), 366–375.

Vinuesa, R., Schlatter, P. & Nagib, H. M. 2015 Characterization of the secondary flow in turbulent rectangular ducts with varying aspect ratio. *Proceedings of the 9th International Symposium on Turbulence and Shear Flow Phenomena, Melbourne, Australia* p. 1–6.

Virk, P. S. 1975 Drag reduction fundamentals. *AIChE Journal* **21** (4), 625–656.

Waleffe, F. 2001 Exact coherent structures in channel flow. *J. Fluid Mech.* **435**, 93–102.

Walker, D. T. & Tiederman, W. G. 1990 Turbulent structure in a channel flow with polymer injection at the wall. *J. Fluid Mech.* **218**, 377–403.

Whalley, R. D., Dennis, D. J. C., Graham, M. D. & Poole, R. J. 2019 An experimental investigation into spatiotemporal intermittencies in turbulent channel flow close to transition. *Exp. Fluids* **In press**.

Whalley, R. D., Park, J. S., Kushwaha, A., Dennis, D. J. C., Graham, M. D. & Poole, R. J. 2017 Low-drag events in transitional wall-bounded turbulence. *Phys. Rev. Fluids* **2**, 034602.

Xi, L. & Graham, M. D. 2010 Active and hibernating turbulence in minimal channel flow of newtonian and polymeric fluids. *Phys. Rev. Lett.* **104**, 218301.

Xi, L. & Graham, M. D. 2012 Intermittent dynamics of turbulence hibernation in newtonian and viscoelastic minimal channel flows. *J. Fluid Mech.* **693**, 433–472.